THE ANNALS OF "DUNAREA DE JOS" UNIVERSITY OF GALATI
FASCICLE IX. METALLURGY AND MATERIALS SCIENCE
Nº. 4 - 2022, ISSN 2668-4748; e-ISSN 2668-4756
Article DOI: https://doi.org/10.35219/mms.2022.4.05

A SENSITIVITY STUDY OF THE MAXIMUM STRESS IN A RUBBER CIRCULAR RING TO THE COEFFICIENT OF FRICTION USING FEM

Doina BOAZU
"Dunarea de Jos" University of Galati, Department of Mechanical Engineering, Romania
e-mail: doina.boazu@ugal.ro

ABSTRACT

The paper presents a sensitivity study of a rubber circular ring (O-Ring) depending on the value of the coefficient of friction (design parameter) between the ring and the surfaces between which it is mounted. The response value is the maximum von Mises stress in the rubber ring. The influence of temperature was not taken into account.

Through this sensitivity nonlinear analysis using finite element modeling, the correlation between Equivalent maximum Von Mises Stress and Friction coefficient can be established, determining a maximum stress level of the rubber ring to the friction coefficient. This relationship is important for the preload stage of the gasket functioning.

KEYWORDS: nonlinear analysis, rubber, contact, axisymmetric PLANE2D, friction

1. Introduction

O-rings are one of the most widely used seals today in industries like automotive, shipping, machinery, energy. They have simple design, easy to manufacture [5]. In the preload stage of functioning, O-ring follows the principle: when compressing an elastomer material between two surfaces, it changes its shape. During this procedure, the material is forced to restore its original shape and as a result, contact pressure is developing [5].

György Szabó and Károly Váradi in [5] investigated the behavior of an O-ring made of NBR rubber under extreme conditions. The effect of the extreme initial compression, operating pressure and extreme temperature conditions were examined.

The stresses in the O-rings made of elastomers have been investigated in recent years, the studies containing both simulations with finite elements and experimental determinations.

George A. F., Strozzi A. and Rich I. in reference [2] developed a finite element stress analysis computer program, FEMALES (an acronym for Finite Element Mechanical Analysis of Large Elastic Strain), at the University of Bologna, Italy. This program was developed specifically for the analysis of large deformations in elastomeric materials.

In [3] the authors studied the stresses and deformations of the compressed elastomeric O-rings, and Jeong-Hwan Nam, Jai-Sug Hawong, Dong-Chul Shin and Bruno R. Mose studied the stresses of O-rings using transparent type photo-elastic experiment [4].

The most common materials used for gaskets are Graphite, Rubber, Teflon, PTFE, and Compressed Non-Asbestos Fiber (CNAF). These are soft gaskets. It can be full face or inside bolt circle type [6, 7].

Non-Metallic gaskets can easily compress with low tension bolting.

These types of gaskets are used with low-pressure and also in low-temperature. However, graphite gasket can be used up to 500 Degree centigrade.

Rubber and elastomer gaskets are not used in hydrocarbon services but used in utility lines.

Non-Metallic gaskets are the cheapest and most easily available.

There are many different types of gaskets and each are classified by material, function, and fields of application. Typically, a gasket is manufactured with a soft, hyper-elastic material and placed between two separate surfaces.

The main types of Rubber Gasket Materials used are:

- Neoprene;

THE ANNALS OF "DUNAREA DE JOS" UNIVERSITY OF GALATI
FASCICLE IX. METALLURGY AND MATERIALS SCIENCE
N°. 4 - 2022, ISSN 2668-4748; e-ISSN 2668-4756
Article DOI: https://doi.org/10.35219/mms.2022.4.05

- Nitrile (Buna-N);
- Ethylene Propylene Diene Monomer (EPDM);
- Silicone Rubber;
- Viton®;
- Styrene Butadiene Rubber (SBR).

2. Material properties of the structural elements

The structural elements and their dimensions are shown in Fig. 1a (according to a scheme presented in [9]). The circular rubber ring of the type shown in Fig. 1b is crushed between the two steel plates.

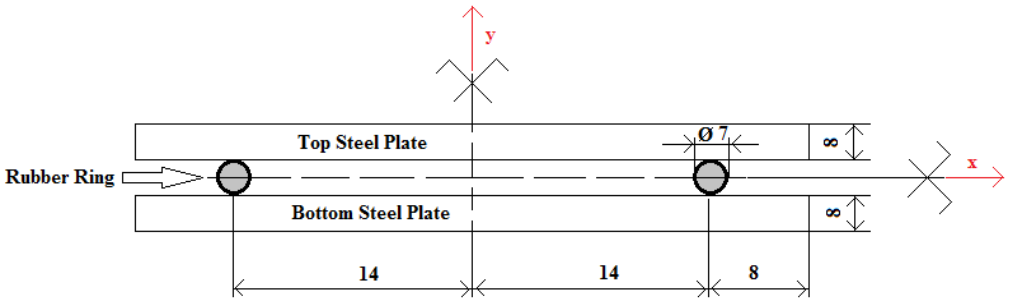

Fig. 1a. *Structural elements of the system* [9]

Fig. 1b. *Neoprene O-ring*

In the non-linear analysis, which involves frictional contact between the steel plates and the rubber ring, the behavior of the material of the steel plates was considered linear elastic (Structural Steel), while for the rubber ring the Neoprene Rubber having Neo-Hookean material model from the library of Ansys Workbench program was chosen (*Initial Shear Modulus Mu = 27104 (Pa) and Incompressibility Parameter D1 = 1.4429E-7 (Pa^-1)*); the Stress-Strain curves for this Neopren rubber is represented in Fig. 2.

The mechanical properties for the material of the Structural Steel plates are:

- Young Modulus 2.1e11 N/m^2;
- Poisson ratio 0.3.

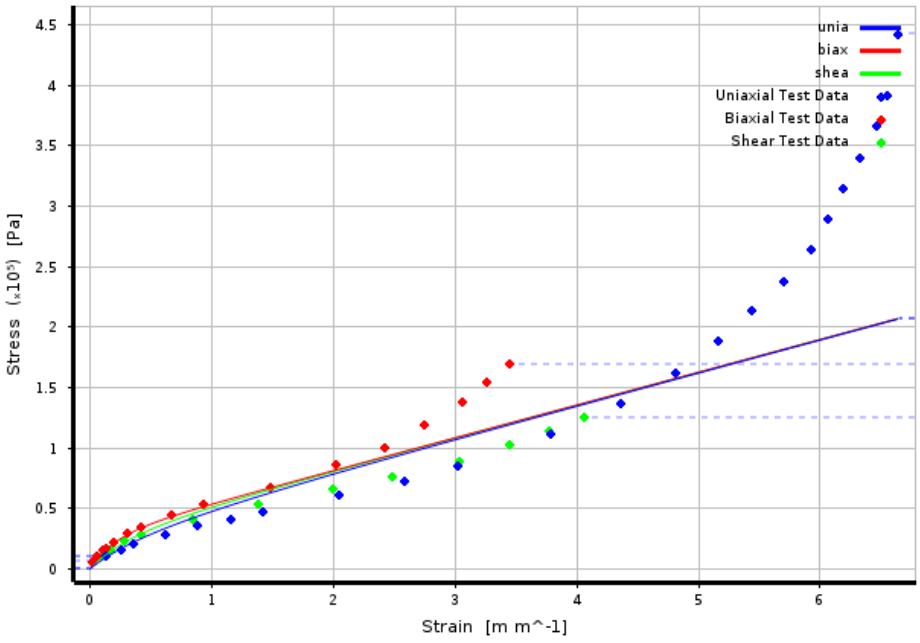

Fig. 2. *Stress-strain curves for Neoprene Rubber* [8]

THE ANNALS OF "DUNAREA DE JOS" UNIVERSITY OF GALATI
FASCICLE IX. METALLURGY AND MATERIALS SCIENCE
Nº. 4 - 2022, ISSN 2668-4748; e-ISSN 2668-4756
Article DOI: https://doi.org/10.35219/mms.2022.4.05

3. Finite element model and parametrization

The nonlinear model was created in the Ansys Workbench version 19.2 program in the Static Structural module.

In this study of sensitivity of circular ring response to the friction coefficient value, the friction coefficient was considered the design variable and the maximum von Mises stress in the rubber ring was considered the response quantity.

The elements of the structure are shown in Fig. 1a. The rubber ring is placed between the two circular steel plates. Due to the double symmetry, the model with finite elements can only be made on a quarter, imposing specific conditions in the planes of symmetry (zero displacements outside the planes of symmetry).

The model can therefore be made on a quarter with axisymmetric 2D elements, imposing *asymmetric* contact conditions with friction between the circular surface of the rubber ring (*Contact*) and the steel plate (*Target*) Fig. 3. Since the contact is made in 2D, it is between a circle and a line and for the non-linear calculation, the option *Interface treatment* > *Adjust to Touch* is activated. For the non-linear calculation, the incremental calculation and large displacement calculation options are activated.

The finite element discretization is presented in Fig. 4.

The finite element used in the discretization is PLANE183 with axisymmetric option (Fig. 5) [8].

Plane183 is a higher order 2D, 8-node per element with has quadratic displacement behavior. This element is more accurate in modeling curved boundaries. The element Plane183 has two DOF – displacement in x and y direction.

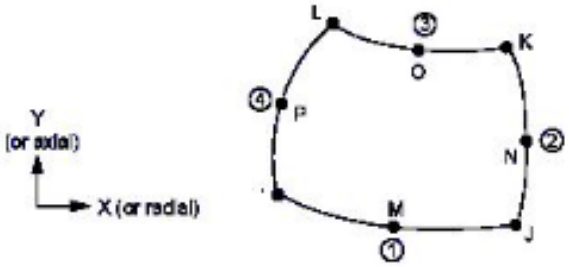

Fig. 5. *The element PLANE183 with axisymmetric option* [8]

For the nonlinear analysis, it is advantageous to apply the load in the form of prescribed displacement (a half of the O-ring radius), the corresponding force being evaluated as a reaction in the imposed boundary.

The boundary conditions are presented in Fig. 6. These boundary conditions are:

- A - Displacement on X direction (radial) – Free and Displacement on Y direction (axial) – Zero;
- B - Displacement on X direction (radial) – Zero and Displacement on Y direction (axial) – Free;
- C - Prescribed displacement on Y direction – 1.5 mm and Displacement on X direction (radial) – Zero.

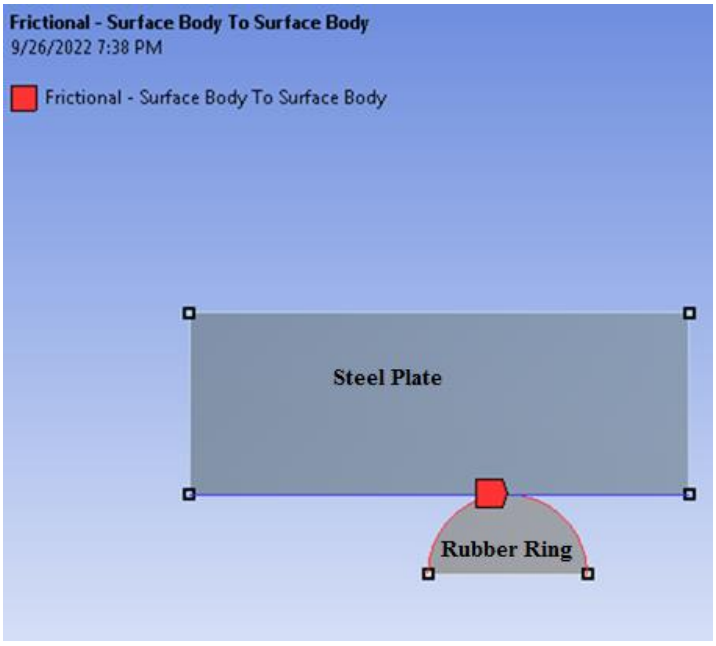

Fig. 3. *Contact surfaces*

THE ANNALS OF "DUNAREA DE JOS" UNIVERSITY OF GALATI
FASCICLE IX. METALLURGY AND MATERIALS SCIENCE
No. 4 - 2022, ISSN 2668-4748; e-ISSN 2668-4756
Article DOI: https://doi.org/10.35219/mms.2022.4.05

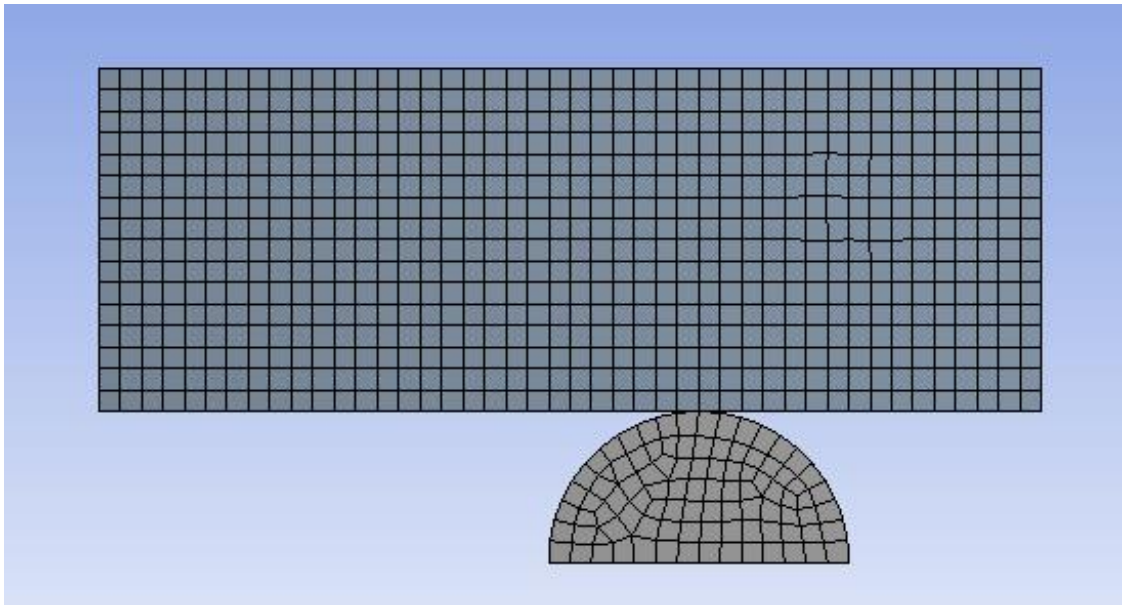

Fig. 5. *Mesh using PLANE183 (size of element 0.5 mm)*

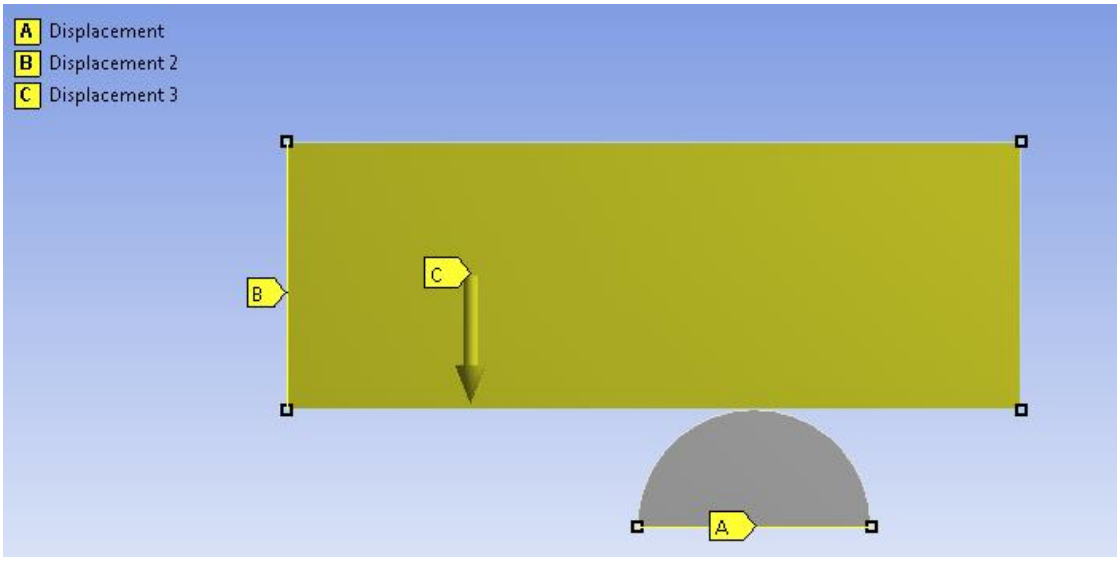

Fig. 6. *Boundary conditions*

4. Results and discutions

The results obtained for the friction coefficient value of 0.01 are presented in Fig. 7 and Fig. 8.

The distribution of total displacements is given in Fig. 7, and the von Mises stress distribution is given in Fig. 8. The maximum stress appears in the centre of the rubber ring.

Schematic Project in the Ansys Workbench analysis program is presented in Fig. 9.

In the sensitivity study, the value of the friction coefficient as a parameter varies between 0.01 and 0.25 (Fig. 10). In Fig. 10 - Design of experiments, both the values of the friction coefficient (variable design) and the corresponding response values of the maximum von Mises stress can be found.

To obtain the Response Surface, the Response Surface Optimization Module was used, and then to obtain the correlation of the parameters, the Parameters Correlations module was used (Fig. 9).

The graphic representation of Equivalent maximum Von Mises Stress vs Friction coefficient is given in the Fig. 11.

The correlation between Equivalent Maximum Von Mises Stress vs Friction coefficient for the linear and quadratic trends has the graphic representation in the Fig. 12, with the correlation functions and the correlation coefficients in Table 1.

THE ANNALS OF "DUNAREA DE JOS" UNIVERSITY OF GALATI
FASCICLE IX. METALLURGY AND MATERIALS SCIENCE
Nº. 4 - 2022, ISSN 2668-4748; e-ISSN 2668-4756
Article DOI: https://doi.org/10.35219/mms.2022.4.05

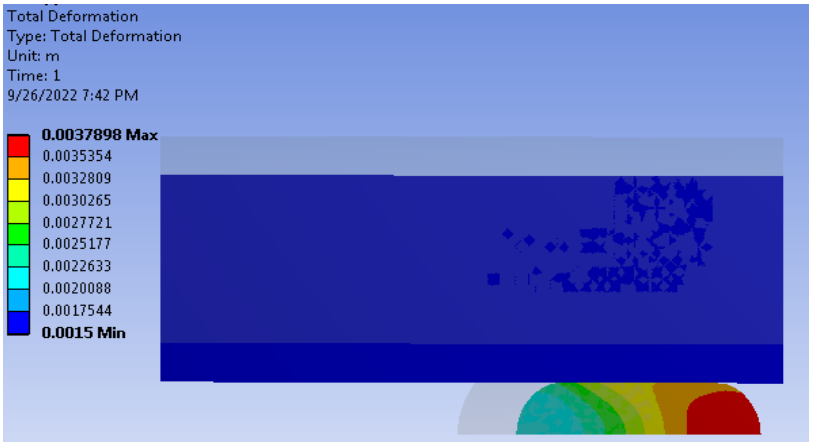

Fig. 7. *Total Deformation distribution (over the initial position)*

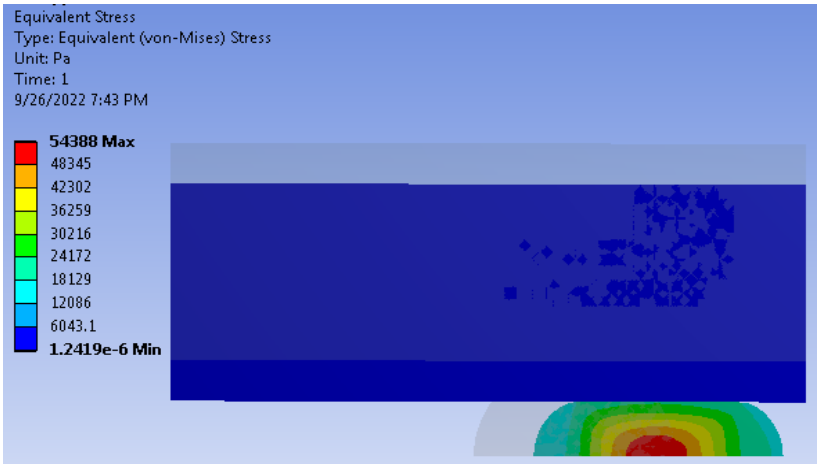

Fig. 8. *Distribution of von Mises stress (over the initial position)*

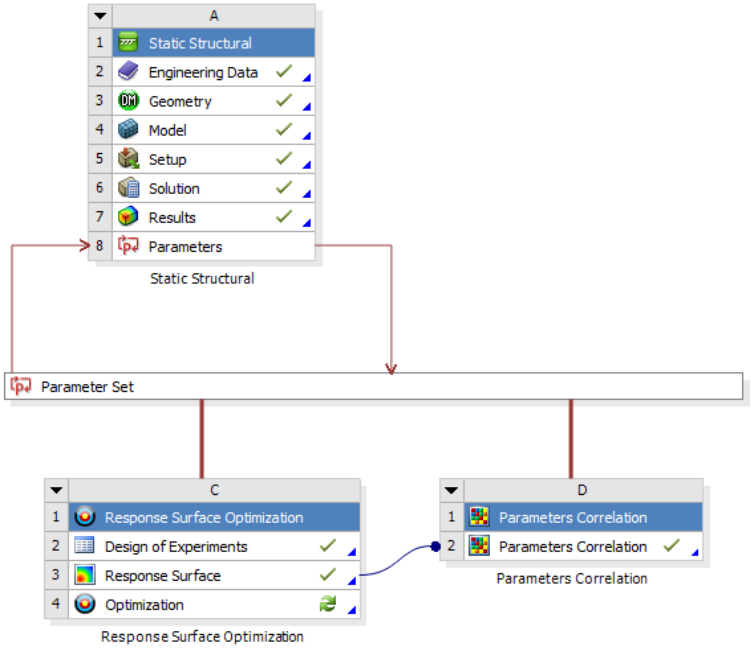

Fig. 9. *Project schematic*

THE ANNALS OF "DUNAREA DE JOS" UNIVERSITY OF GALATI
FASCICLE IX. METALLURGY AND MATERIALS SCIENCE
Nº. 4 - 2022, ISSN 2668-4748; e-ISSN 2668-4756
Article DOI: https://doi.org/10.35219/mms.2022.4.05

Table of Outline A2: Design Points of Design of Experiments

	A	B	C
1	Name	P1 - Frictional - Surface Body To Surface Body Friction Coefficient	P2 - Equivalent Stress 2 Maximum (Pa)
2	1 DP 0	0.01	54388
3	2 DP 1	0.05	64085
4	3 DP 2	0.09	79608
5	4 DP 3	0.13	90890
6	5 DP 4	0.17	99057
7	6 DP 5	0.21	1.0493E+05
8	7 DP 6	0.25	1.0783E+05
*	New Design Point		

Fig. 10. *Design of experiments*

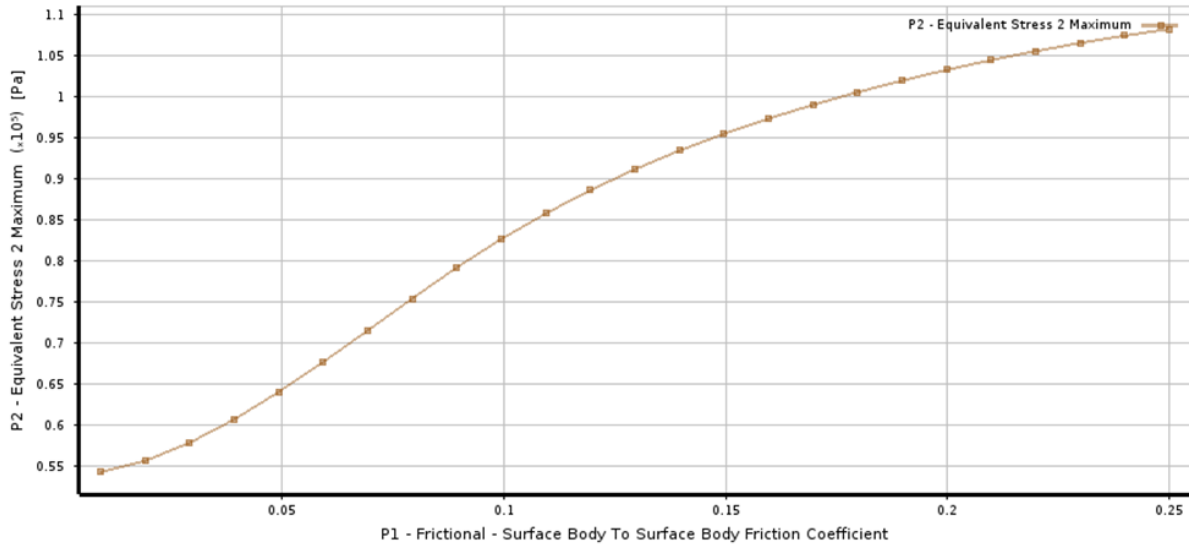

Fig. 11. *Equivalent maximum Von Mises Stress vs Friction coefficient*

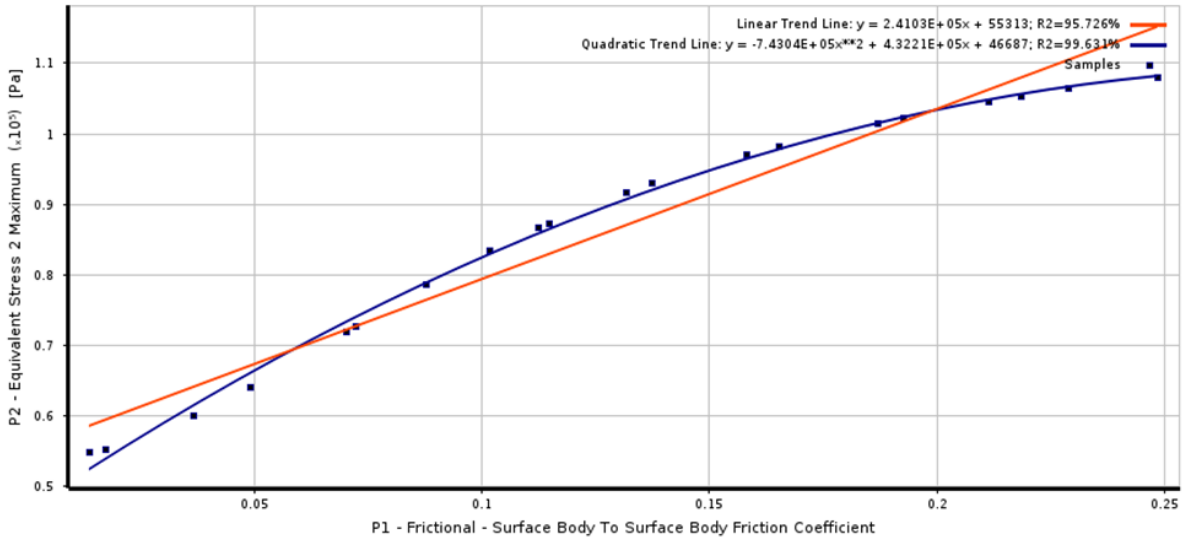

Fig. 12. *Correlation Equivalent maximum Von Mises Stress "y" vs Friction coefficient "x" for linear and quadratic trends*

THE ANNALS OF "DUNAREA DE JOS" UNIVERSITY OF GALATI
FASCICLE IX. METALLURGY AND MATERIALS SCIENCE
N°. 4 - 2022, ISSN 2668-4748; e-ISSN 2668-4756
Article DOI: https://doi.org/10.35219/mms.2022.4.05

Table 1. *Trend lines for sensitivity study*

Trend Lines	Function	Correlation
Linear	$y = 2.41e5 * x + 55313$	R = 95.726%
Quadratic	$y = -7.43e4 * x^2 + 4.322e5 * x + 46687$	R = 99.631%

5. Conclusions

If the material curves for the O-ring are known, the dependence curves of Equivalent maximum Von Mises Stress vs Friction coefficient can be obtained from the sensitivity analysis with finite elements.

Having the dimensions of the elements of the system and the value of the coefficient of friction between the O-ring and the steel surface and performing a sensitivity analysis, the maximum von Mises stresses in the centre of the O-ring can be established.

A better correlation function between Equivalent maximum Von Mises Stress and the Friction coefficient is that corresponding to quadratic trend (Table 1) and this relationship is very important for the preload stage of the O-ring loading.

The maximum von Mises stress for this preload stage of loading of the O-ring should be below the value of 25 MPa.

References

[1]. Brice N., Cassenti Alexander Staroselsky, *Deformation and stability of compressible rubber O-rings*, International Journal of Mechanical and Materials Engineering, vol. 12, article number: 5, 2017.
[2]. George A. F., Strozzi J. A., Rich I., *Stress fields in a compressed unconstrained elastomeric O-ring seal and a comparison of computer predictions and experimental results*, Tribology International, vol. 20, issue 5, p. 237-247, October 1987.
[3]. Itzhak Green, Capel English, *Stresses and deformation of compressed elastomeric O-ring seals*, 14th International Conference on Fluid Sealing, Firenze, Italy, 6-8 April 1994.
[4]. Jeong-Hwan Nam, Jai-Sug Hawong, Dong-Chul Shin, Bruno R. Mose, *A study on the behaviors and stresses of O-ring under uniform squeeze rates and internal pressure by transparent type photoelastic experiment*, Journal of Mechanical Science and Technology, 25 (9), DOI: 10.1007/s12206-011-0713-4, 2011.
[5]. György Szabó, Károly Váradi, *Failure Mechanism of O-Ring Seals under Extreme Operating Conditions*, Modern Mechanical Engineering, vol. 8, no. 1, February 2018.
[6]. ***, https://www.linkedin.com/pulse/main-causes-failure-o-ring-seals-permanent-lisa.
[7]. ***, https://www.callapg.com/blog-the-9-most-common-types-of-gaskets.
[8]. ***, *Ansys Workbench*, version 19.2 documentation.
[9]. ***, Cosmos/M, version 2.7 documentation.